

Sulforhodamine 101 as a specific marker of astroglia in the neocortex *in vivo*

Axel Nimmerjahn¹, Frank Kirchhoff², Jason N D Kerr¹ & Fritjof Helmchen¹

Glial cells have been identified as key signaling components in the brain; however, methods to investigate their structure and function *in vivo* have been lacking. Here, we describe a new, highly selective approach for labeling astrocytes in intact rodent neocortex that allows *in vivo* imaging using two-photon microscopy. The red fluorescent dye sulforhodamine 101 (SR101) was specifically taken up by protoplasmic astrocytes after brief exposure to the brain surface. Specificity was confirmed by immunohistochemistry. In addition, SR101 labeled enhanced green fluorescent protein (EGFP)-expressing astrocytes but not microglial cells in transgenic mice. We used SR101 labeling to quantify morphological characteristics of astrocytes and to visualize their close association with the cortical microvasculature. Furthermore, by combining this method with calcium indicator loading of cell populations, we demonstrated distinct calcium dynamics in astroglial and neuronal networks. We expect SR101 staining to become a principal tool for investigating astroglia *in vivo*.

Glial cells have for a long time been considered as pure supporting elements in nervous tissue, but evidence has accumulated that a tight, bidirectional communication exists between neurons and glial cells, suggestive of a key role of glia in signal processing in the CNS (for reviews see refs. 1–3). A multitude of signaling tasks is proposed for astroglia, including the modulation of synaptic function^{4–6}, long-range signaling^{7,8} and cerebral blood-flow regulation^{9,10}. Most studies, however, have been carried out in cultured cells or brain slice preparations and thus the relevance of astroglial signaling *in vivo* remains unclear. Hence, there has been a call for techniques to enable *in vivo* studies of astrocyte structure and function in the intact brain^{3,11}.

Owing to its exceptional depth penetration and intrinsic optical sectioning properties, two-photon-excited fluorescence laser scanning microscopy¹² has become the principal technique for high-resolution *in vivo* imaging. It has been used to study tissues as diverse as brain, skin, lymph nodes and tumors (for reviews see refs. 13–15). Although neocortical neurons have been investigated extensively using various approaches^{16–19}, tools allowing observation of glial cells *in vivo* are just emerging. For example, transgenic mice have been generated with enhanced green fluorescent protein

(EGFP) expression in astrocytes^{20,21} or microglia²². However, no simple staining method has been available so far that would allow the specific labeling of astroglia in the intact neocortex of rodents.

Here we demonstrate a new and robust method for fluorescently labeling astroglia *in vivo* by briefly exposing the neocortical surface to the red fluorescent dye sulforhodamine 101 (SR101). We provide several lines of evidence that SR101 is specifically taken up by protoplasmic astrocytes. Using *in vivo* two-photon microscopy, we visualized the distribution of astrocytes in neocortex down to a depth of 700 μm . In addition, by combining SR101 labeling with bulk calcium indicator loading, we were able to simultaneously measure calcium dynamics in both astroglial and neuronal networks.

RESULTS

SR101 labels a subpopulation of neocortical cells *in vivo*

Brief exposure of the neocortex of anesthetized rats and mice to the red fluorescent SR101 resulted in rapid staining of a subpopulation of neocortical cells (Fig. 1). Using *in vivo* two-photon microscopy, SR101-labeled cells were imaged down to 700 μm below the pial surface, revealing a relatively homogenous, non-layered distribution (Fig. 1b and Supplementary Video 1). Only a fraction of cells took up SR101, as indicated by the many unstained cell bodies found particularly in layer 2 and deeper (Fig. 1a). All SR101-labeled cells had similar morphological features with multiple processes originating from the cell body, often forming end feet-like structures attached to (unstained) blood vessels. Thus, their morphology closely resembled that of protoplasmic astrocytes as described for neocortex²³.

We typically obtained bright SR101 labeling using micromolar concentrations and extracellular application for several minutes. However, concentrations as low as 250 nM, and dye exposure times as short as a few seconds, were sufficient. SR101 labeling was stable for several hours, with only a slow decay in fluorescence intensity. Over this time course a more granular staining pattern developed, indicating sequestration of SR101 into intracellular organelles. To measure the time course of SR101 uptake, we applied SR101 intracortically through brief (3 s) pressure ejection from a micropipette (borosilicate glass, 2.0-mm outer diameter; 4–7-M Ω tip resistance). Close to the pipette tip, several cells were gradually stained within a few minutes and reached stable fluorescence levels after about 10 min (Fig. 1c). Notably, 60 min after local application,

¹Abteilung Zellphysiologie, Max-Planck Institut für medizinische Forschung, Jahnstr. 29, 69120 Heidelberg, Germany. ²Abteilung Neurogenetik, Max-Planck Institut für experimentelle Medizin, Hermann-Rein-Str. 3, 37075 Göttingen, Germany. Correspondence should be addressed to F.H. (fritjof@mpimf-heidelberg.mpg.de).

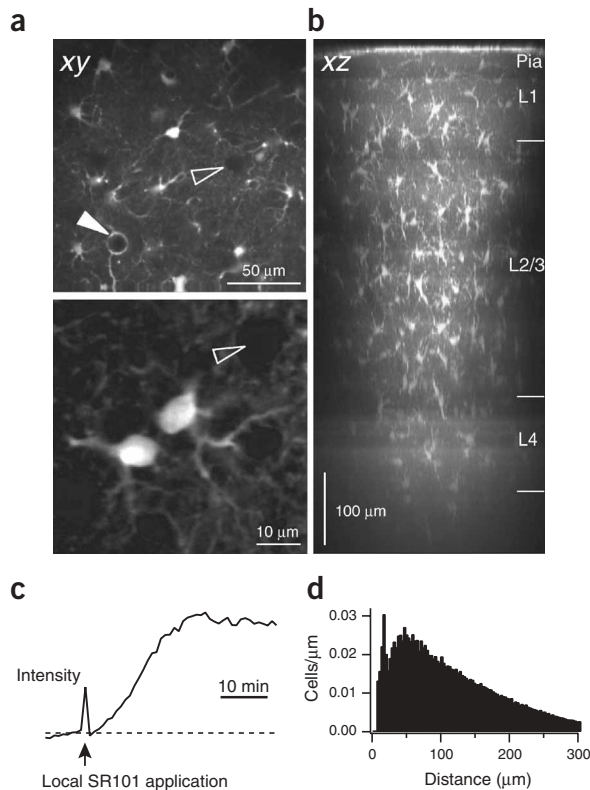


Figure 1 | *In vivo* staining pattern of neocortical cells after application of SR101. (a) Two-photon fluorescence images (individual focal planes). Top, overview recorded about 200 μm below the pial surface, showing that a subpopulation of cells had taken up the dye. Blood vessels (solid arrowhead) and unstained cell bodies (open arrowhead) appeared as dark gaps. Bottom, high-magnification image of a labeled cell pair. (b) Overview side projection of an SR101-stained area in mouse neocortex ~ 30 min after dye application. The image is a maximum-intensity side-projection from a stack of fluorescence images. (c) Time course of dye loading after brief intracortical dye ejection (3-s pressure pulse, 0.7 bar; 250 nM SR101 in extracellular saline). Fluorescence intensity was averaged for three cells that appeared next to the application pipette. (d) Radial density distribution of astrocytes in the intact mouse brain. Note sharp peak at a mean cell-to-cell distance of ~ 15 μm , which corresponds to frequently observed pairs of astrocytes in very close proximity.

labeled cells showing comparable levels of fluorescence could be found in the entire cranial window (1–2 mm in diameter). This suggests that the spread of dye is supported by gap-junctional connections between SR101-labeled cells. Indeed, local application of the gap-junction blocker carbenoxolone (CBX, 100 μM ; Sigma-Aldrich) markedly suppressed labeling of topically applied SR101 near the application pipette in a concentration-dependent manner (Fig. 2). Furthermore, CBX applied topically, as part of the objective immersion medium, delayed the spread of locally applied SR101 (data not shown).

In summary, a wide range of SR101 concentrations and exposure times resulted in robust and rapid labeling of neocortical cells. On the basis of their morphology and their gap-junctional coupling, these cells appeared to be protoplasmic astrocytes.

SR101 specifically stains neocortical protoplasmic astrocytes

The specificity of SR101-labeling for astrocytes was verified using immunohistochemistry. Because SR101 tends to leak out of cells in

fixed tissue²⁴, we used the paraformaldehyde-fixable analog Texas Red–hydrazone, which resulted in a staining pattern similar to that from SR101. After *in vivo* staining with Texas Red–hydrazone, vibratome sections of labeled tissue were counter-immunostained for the calcium-binding protein S-100 β , a specific marker of astrocytes²⁵. Nearly all SR101-analog stained cells were found to be S-100 β positive (Fig. 3a; Supplementary Table 1; $95.1 \pm 1.1\%$; $n = 520$ total cells, 4 animals; 0.4% of S-100 β -positive cells presumably were SR101 negative).

By counter-immunostaining for the enzyme CNPase, which is specifically expressed in oligodendrocytes in the CNS, we also tested whether oligodendrocytes might take up SR101 (Fig. 3b). Nearly all CNPase-positive cells were SR101 negative, with only very few exceptions (15 of 565 total cells, in 4 animals, showed some overlap). Finally, counter-immunostaining for the neuron-specific nuclear protein NeuN showed no overlap between the two cell populations (Fig. 3c; zero overlap; $n = 554$ total cells; 3 animals). These results indicate that SR101 is selectively taken up by protoplasmic astrocytes when applied *in vivo*.

SR101 labels protoplasmic astrocytes but not microglial cells

We further confirmed the astroglial specificity of SR101 uptake in experiments using transgenic mice that express EGFP in either astrocytes or microglia. We first applied SR101 to the cortex of transgenic mice (TgN(GFAP-EGFP)) in which the human glial fibrillary acidic protein (hGFAP) promoter controls EGFP expression. Only a fraction of neocortical astrocytes express EGFP in these mice²¹. In five animals tested, nearly all EGFP-expressing astrocytes ($97.2 \pm 1.9\%$; $n = 1,064$ total cells) were colabeled by SR101 (Fig. 4a, upper row; Supplementary Video 2 and Supplementary Table 2). The few exceptions (17 of 1,064 total cells) were weakly EGFP-expressing cells. These cells most likely represent a subpopulation of astrocytes^{25,26} that previously have also been described as glial progenitor cells²⁷, and that are immunopositive for proteoglycan NG2²⁶ and are not coupled by gap junctions²⁸. In addition to the nearly complete overlap with EGFP-expressing cells, SR101 labeled many more cells showing similar morphology (Fig. 4a, upper row). In total, about half of the SR101-labeled cells were EGFP positive ($52 \pm 3\%$; $n = 2,034$ total cells; 5 animals). The EGFP-negative cells presumably represent the fraction of cortical astrocytes in which the GFAP-EGFP transgene was not active.

To examine whether microglial cells take up SR101, we took advantage of another genetically modified mouse line, in which the EGFP reporter gene is inserted into the *Cx3cr1* locus, encoding the chemokine receptor CX₃CR1 (also known as the fractalkine receptor)²². This genetic modification causes specific EGFP expression in resident microglial cells as well as macrophages. Microglial cells had anatomical features distinct from those of protoplasmic astrocytes, showing small rod-shaped somata from which numerous thin processes extended symmetrically²⁹. Microglial cells and astrocytes could therefore be readily distinguished by their morphology. Consistent with this notion, we found that SR101 is not taken up by microglial cells, as indicated by lack of overlap between EGFP-expressing microglia and SR101-labeled astrocytes (Fig. 4a, lower row; Supplementary Video 3). The few exceptions found in the CX₃CR1-EGFP mice (3 of 638 total cells; 3 animals) appeared to be resident macrophages.

Based on immunohistochemistry and comparison of staining patterns in transgenic mice, we concluded that SR101 is specifically

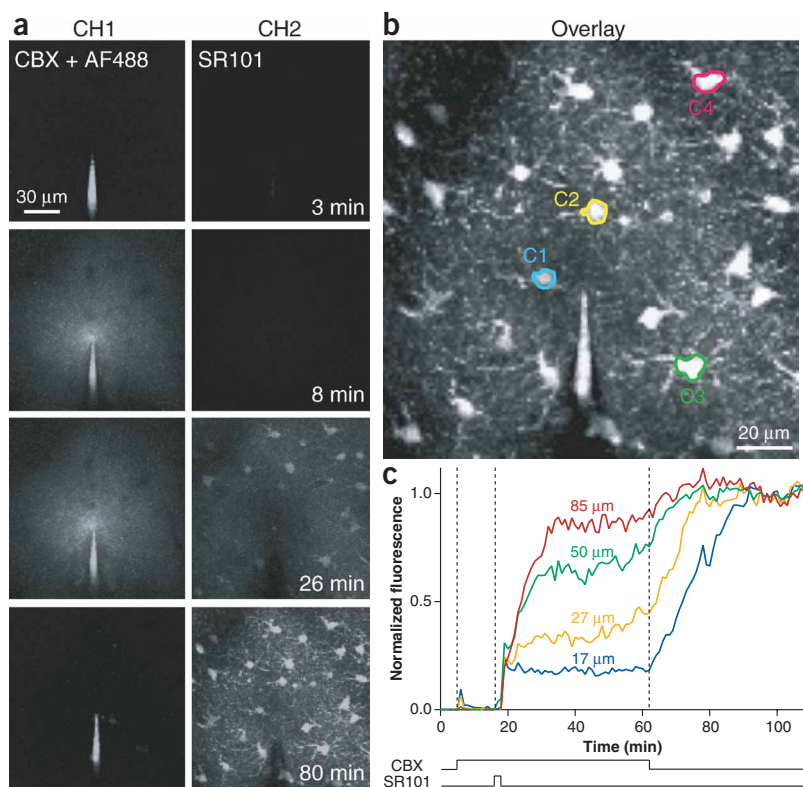


Figure 2 | Gap junctions permit rapid spread of SR101. The gap-junction blocker carbenoxolone (CBX; 100 μM) was applied through a micropipette 85 μm below the pial surface. The pipette solution also contained the green fluorescent dye Alexa Fluor 488 (AF488; 100 μM) as a means to visualize the pipette shank and CBX ejection. During CBX application, SR101 was briefly applied to the cortical surface, which was then rinsed twice. At 45 min after SR101 application, CBX pressure ejection was ceased. **(a)** Sample images from the dual-channel *in vivo* time-lapse recording (taken at 60-s intervals). Images in left and right columns show the CBX-containing micropipette detected in the green channel (CH1) and the fluorescence detected in the red channel (CH2), respectively. Acquisition times are indicated for each row. Each image is a maximum-intensity projection of a $132 \times 132 \times 48 \mu\text{m}^3$ fluorescence image stack ($3\text{-}\mu\text{m}$ axial spacing). **(b)** Overlay of red and green fluorescence channel images indicating the micropipette tip position in two dimensions relative to surrounding cells. **(c)** Time course of fluorescence intensities in the regions of interest indicated in **b**. Intensities were normalized to their final values. Numbers above the curves indicate the radial distances of each cell from the micropipette tip in three dimensions. Periods of local CBX and topical SR101 application are indicated in lower traces.

taken up by protoplasmic astrocytes in neocortex of both rats and mice.

Morphological characteristics of neocortical astroglia

Using SR101 staining, we analyzed *in vivo* distribution of neocortical astrocytes in detail. Consistent with the territorial organization of protoplasmic astrocytes^{11,29}, this distribution was rather homogeneous. Volume densities ranged from 14×10^3 to 28×10^3 cells/ mm^3 , with an approximately 55% higher density in layer 1 than in layer 2/3 (Table 1). In general, astrocyte densities in rats were about 25% higher than in mice. We also analyzed volume densities of microglial cells in CX₃CR1-EGFP mice, which were about 30–50% of those of SR101-labeled cells ($7.9 \pm 0.8 \times 10^3$ cells/ mm^3 and $7.8 \pm 0.6 \times 10^3$ cells/ mm^3 in layer 1 and layer 2/3, respectively; $n = 3$ animals). Furthermore, we analyzed the average radial density of SR101-labeled cells surrounding individual astrocytes (Fig. 1d). Distances between neighboring cell bodies were around 50 μm . The distribution also showed a distinct peak at a mean cell-to-cell distance of approximately 15 μm , corresponding to the frequent observation of pairs of astrocytes whose cell bodies were separated by only a small gap in extracellular space. These pairs constituted 10–15% of all SR101-labeled cells ($13.5 \pm 1.2\%$ for rats, $n = 8$ animals; $9.9 \pm 1.3\%$ for mice, $n = 7$ animals; see Fig. 1a and Fig. 4a for examples).

Time-lapse imaging experiments of up to 10 h showed that SR101-labeled cells were morphologically stable, showing no signs of acute phototoxicity such as disintegration of cellular processes (Supplementary Fig. 1a). Furthermore, in TgN(GFAP-EGFP) mice, astrocytes showed no changes in morphology after multiple repeat SR101 application (500 μM) and imaging for up to 3 weeks (Supplementary Fig. 1b). The exact same cells could be found in

successive imaging sessions. In particular, the pairs of astrocytes described earlier remained morphologically unaltered over this time period. In addition, the same staining pattern was observed after repeated SR101 applications (Supplementary Fig. 1c). These short- and long-term imaging experiments demonstrated that SR101 does not induce phototoxicity over hours, days and weeks and can be applied repeatedly.

Astrocytes form a functional, gap junction-coupled syncytium that is closely associated with microvasculature, presumably controlling extracellular milieu and regulating local blood flow^{9,10}. We were able to demonstrate this close apposition to cortical microvasculature by labeling astrocytes with SR101 and counterstaining the blood plasma with a green fluorescent dye via tail-vein injection. Using this approach, we obtained *in vivo* visualization of the entire cortical microvasculature being enveloped by processes of SR101-labeled cells (Fig. 4b; Supplementary Video 4). The endothelial sheet surrounding the blood vessels was visible as an unstained dark gap between astrocyte end feet and fluorescently labeled vessel lumen (Fig. 4b). The complete envelopment of microvasculature provides further evidence that all protoplasmic astrocytes are labeled by SR101 near the application site.

These examples demonstrate how SR101 labeling can be used in both short- and long-term studies to characterize morphological features of astrocytes as well as their close structural relationship to other cortical elements *in vivo*.

Functional imaging of astroglial and neuronal Ca²⁺ signaling

Astrocytes form a cellular network that is closely associated with neuronal networks³. Changes in intracellular calcium levels are thought to be a prominent signaling mechanism not only between astrocytes but also for the communication between astrocytes and

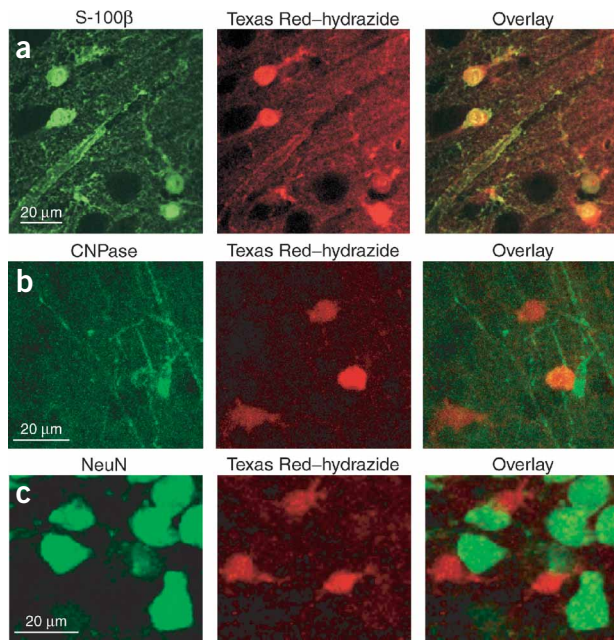


Figure 3 | SR101-labeled cells are immunopositive for S-100 β protein, but not for either the neuron-specific nuclear protein NeuN or, in the vast majority of cases, the enzyme CNPase *in vitro*. (a) Left, Pacific Blue fluorescence of anti-S-100 β -labeled astrocytes in the green detection channel. Center, red fluorescence of cells stained with Texas Red-hydrizide, a paraformaldehyde-fixable analog of SR101. Right, overlay of green and red fluorescence channels. (b) Left, Pacific Blue fluorescence of an oligodendrocyte labeled with anti-CNPase. Center, red fluorescence of cells stained with Texas Red-hydrizide. Right, overlay of the green and red fluorescence channels. (c) Left, FITC fluorescence of neurons labeled with anti-NeuN in the green detection channel. Center, cells stained with Texas Red-hydrizide. Right, overlay of the fluorescence images.

neurons^{1,30,31}. Although slow Ca²⁺ oscillations^{32,33} and Ca²⁺ waves^{7,8,32} have been characterized in cell culture and brain slices, the presence and characteristics of such signals *in vivo* have not been clearly established (but see ref. 34).

Using SR101 as a specific marker for astrocytes, we were able to distinguish calcium signals unambiguously in the astroglial and neuronal network *in vivo*. For calcium-indicator loading of cell populations, we used multicell bolus loading¹⁸ with Oregon Green 488 BAPTA-1 acetoxymethyl (AM) ester (OGB-1 AM), which resulted in the staining of virtually all cells within a sphere several hundred microns in diameter. After 30 min, all cells near the ejection site, including neurons and astrocytes, had taken up the calcium indicator (Fig. 5a). Although glial cells sometimes could be recognized because of a higher fluorescence intensity¹⁸, a complete separation of neurons and astrocytes was not possible based on their appearance. Astrocytes, however, could be identified through additional staining with SR101 (Fig. 5a). Because the red fluorescence of SR101 can be easily separated from the green fluorescence of OGB-1, the red fluorescence channel can serve as a reference image to identify astrocytes (Fig. 5b).

Figure 4 | *In vivo* colabeling in neocortex using SR101. (a) SR101 labels astrocytes but not microglial cells in transgenic mice *in vivo*. Upper row: Left, astrocytes expressing EGFP under control of human GFAP promoter in a transgenic mouse line. Center, labeled cells in the same region after surface application of the red fluorescent dye SR101. Right, overlay of the green and red channel. Note that not all SR101-labeled astrocytes show green fluorescence, as the GFAP-EGFP transgene is not active in all cortical astrocytes. Lower row: Left, EGFP-expressing microglial cells in mutant mice. Center, red fluorescent cells in the same region after surface application of SR101. Right, overlay of the green and red channel. (b) SR101 can be used to visualize astrocytic processes such as those found at the gliovascular interface. Example images showing costaining of neocortical astroglia and microvasculature *in vivo*. Blood plasma was stained by tail-vein injection of FITC-labeled dextran. Note that green and red pseudocolor lookup tables were assigned to fluorescence images of SR101 labeled astrocytes and fluorescent labeled blood plasma, respectively.

We monitored spontaneous calcium signals in cortical layer 2/3 cells over several minutes at a temporal resolution of 15 Hz. Spontaneous calcium transients occurred in both neurons and astrocytes; however, they showed markedly different kinetics (Fig. 5c). Astroglial calcium signals were characterized by slow onsets of about 10 s (10–90% rise time 13.2 ± 6 s) and subsequent plateau-like elevations that lasted for several tens of seconds (half width 19.0 ± 2.4 s; $n = 6$). They often showed an oscillatory behavior, occurring repeatedly in individual astrocytes. Calcium signals were not necessarily synchronized between astrocytes. Rather, calcium elevations in some cases appeared to propagate from one astrocyte to neighboring cells in a wave-like fashion (Fig. 5c). In contrast, neuronal calcium signals were characterized by fast fluorescence transients (mean $\Delta F/F$ peak amplitude $11.2 \pm 2\%$, $n = 4$) with a single-exponential decay and a time constant of 0.37 ± 0.05 s ($R^2 = 0.98$, $n = 4$). These transients are consistent with somatic calcium influx evoked by action potentials^{16,35} and therefore can be used to deduce an estimate of the neuronal spike patterns (Fig. 5c). There was no significant difference between neuronal calcium transients from preparations stained with both SR101 and OGB-1 and preparations that were stained with OGB-1 alone ($P = 0.87$).

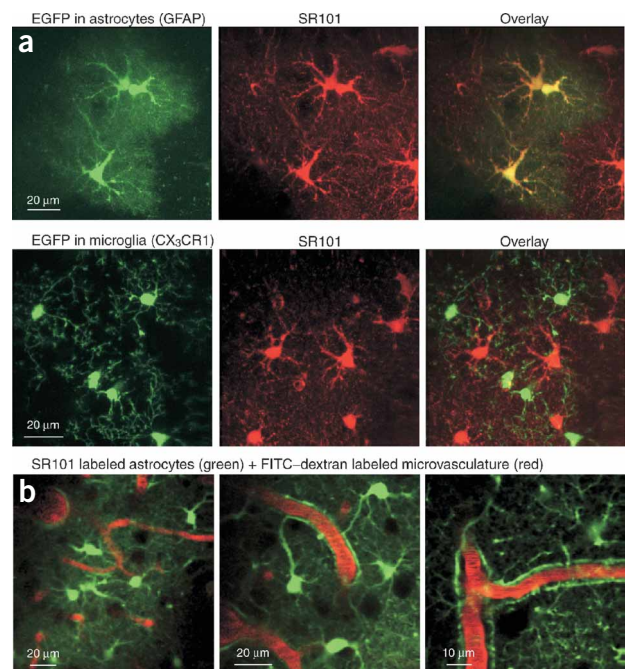


Table 1 | Density of SR101-labeled astrocytes in rat and mouse neocortex (mean \pm s.e.m.)

	Layer 1 (10^3 cells/mm 3)	Layer 2/3 (10^3 cells/mm 3)
Rat (P13–P28)	28.1 \pm 1.2 ($n = 8$ animals)	17.9 \pm 1.4 ($n = 8$ animals)
Mouse (P23–P270)	22.5 \pm 2.0 ($n = 7$ animals)	14.2 \pm 1.1 ($n = 7$ animals)

Thus, SR101 application in conjunction with calcium indicator loading permits simultaneous measurements of neuronal spiking activity and glial calcium signaling *in vivo*. This method should therefore enable *in vivo* studies of the interdependence of glial and neuronal signaling.

DISCUSSION

We have presented here a robust method for labeling neocortical protoplasmic astrocytes *in vivo* through brief exposure of the intact brain to the red fluorescent dye sulforhodamine 101. The specificity of SR101 labeling for astroglia was verified by immunohistochemistry and by applying SR101 in transgenic mice that express EGFP in different glial cell types. We have used this staining method for a morphometric analysis of the distribution of neocortical astrocytes, for visualization of complete glial envelopment of cortical microvasculature, and for dissection of distinct calcium dynamics in astroglial and neuronal networks.

Specific uptake of SR101 by glial cells has been previously reported for rabbit retina²⁴, in which intravitreal application of SR101 caused specific, robust labeling of a subpopulation of cells that were identified as oligodendrocytes. In contrast, we did not find preferential uptake by neocortical oligodendrocytes, as confirmed by counter-immunostaining for CNPase. This difference indicates that the uptake of SR101

varies in different regions and needs to be assessed for each particular brain area. For example, we did not find SR101 uptake by Bergmann glia in cerebellum *in vivo*. A number of *in vitro* studies have reported activity-dependent SR101 uptake in presynaptic terminals³⁶ and neurons³⁷. In both our *in vivo* and counter-immunostaining experiments, there was no indication of activity-dependent uptake in neocortical neurons, although they are known to be spontaneously active^{38,39}. The very few, exceptional cases where SR101 stained additional cells other than protoplasmic astrocytes might represent uptake by macrophages or a specific subtype of oligodendrocytes.

The mechanism of SR101 uptake by astrocytes is not known. Although previous studies of activity-dependent uptake presumed that endocytosis is the predominant mechanism^{36,37}, the efficacy and rapid time course of SR101 loading into neocortical astrocytes, together with the initial homogenous cytoplasmic staining, suggest that a specific transporter system acts as the uptake mechanism²⁴. Furthermore, we found that SR101 spreads through gap junctions, consistent with the gap-junctional spread of other fluorescent dyes of similar size and charge⁴⁰. So far, we have not observed any damaging effects of SR101 on astrocytes or other cortical cells, as indicated by normal cell morphologies after repeated SR101 applications and repeated imaging sessions (for

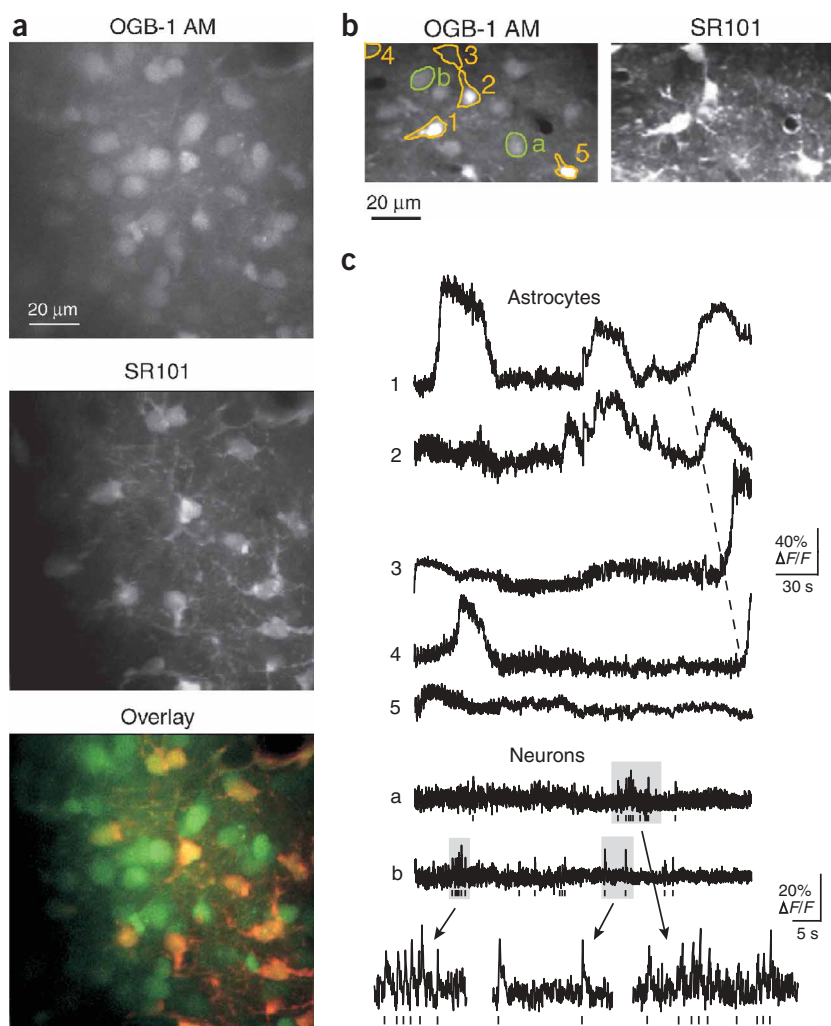


Figure 5 | Simultaneous calcium imaging of neuronal and glial networks *in vivo*. (a) Two-photon fluorescence images of cells in layer 2/3 of rat neocortex labeled by intracortical pressure ejection of the membrane-permeant calcium indicator dye OGB-1 AM (top). Astrocytes were identified through additional surface application of 100 μ M SR101 (center), which permitted a clear separation of the astroglial (yellow) and neuronal (green) network (overlay, bottom). (b) Left, OGB-1 AM-labeled cells in a different experiment. Right, corresponding SR101 reference image for astrocyte identification. Astrocytes and neurons are indicated with numbers and lower-case letters, respectively. (c) Spontaneous calcium transients in the astrocytes and neurons indicated in **b** measured as relative fluorescent change $\Delta F/F$ over a time course of several minutes. Neuronal calcium transients during the highlighted periods are shown on an expanded time scale (bottom traces). Presumed spike patterns are indicated as raster plots below the traces. Note the different time courses of the astroglial and neuronal transients.

several hours and up to 3 weeks) as well as by the unperturbed calcium signaling.

Three findings indicate that SR101 selectively labels all protoplasmic astrocytes in the vicinity of the application site. First, cortical microvasculature was completely enveloped by end feet of SR101-labeled astrocytes. Second, gap junctions are involved in rapid spread of the dye. Third, distribution and densities of SR101-labeled cells in upper layers of cortex are in agreement with previous results *in situ*²⁹. SR101 labeling thus might enable the study of changes in density and distribution of astrocytes *in vivo*, for instance in mouse models of neurodegenerative diseases⁴¹. In addition, colabeling of associated cortical elements, such as blood vessels and neurons, should enable studies of structural plasticity at the gliovascular and the neuron-glia interface, respectively. Counterstaining of blood plasma might be particularly useful when investigating the role of astrocytes in blood-brain barrier integrity⁴¹. Colabeling of neuronal structures, for example by combining SR101 application with viral infection^{17,42} or using transgenic mice⁴³, will make it possible to address the role of astrocytes at the synaptic level *in vivo*. In particular, simultaneous time-lapse imaging of astroglial processes with pre- and postsynaptic structures may help to elucidate their contribution to synapse formation at the tripartite synapse⁴⁴.

We also combined SR101 labeling with bulk loading of membrane-permeable calcium indicators¹⁸, which enabled the simultaneous functional measurement of astroglial and neuronal network dynamics in the living animal. Accumulating evidence suggests that communication between astrocytes and neurons is bidirectional^{1,3}. In particular, astrocytes can release glutamate in a calcium-dependent manner^{45,46} and thus influence neuronal signaling pathways^{1,30,31}. *In vitro*, astrocytic calcium signals have been found in the form of slow calcium elevations as well as calcium waves^{7,8,32}, which can propagate among astrocytes over long distances. The physiological relevance of these calcium oscillations^{32,33} and waves is, however, still unclear. Our results provide direct evidence that astrocytic calcium oscillations and waves do occur *in vivo*. The kinetics of these spontaneous signals was markedly different from those of the fast calcium transients observed in neurons, which were consistent with action potential-induced somatic calcium influx³⁵. This methodological approach for *in vivo* calcium imaging is thus well suited to correlate the activities in neuronal and astroglial networks and is expected to provide new insights into neuron-glia communication as well as into the role of astrocytes in activity-dependent regulation of cerebral blood flow^{9,10}.

In conclusion, the SR101 staining method described here permits a robust and specific labeling of astroglia in the intact brain. We expect this method to be highly beneficial in a multitude of *in vivo* investigations of astroglial structure and function, both in basic research and in more clinically oriented studies.

METHODS

Animals and surgical preparation. All experimental procedures were carried out according to the animal welfare guidelines of the Max-Planck Society. Rats (postnatal day (P) 13–28; Wistar) and mice (P32–272; C57BL6 wild-type or transgenic mouse lines with various genetic backgrounds) were used for experiments. Transgenic animals used in this study included mice expressing EGFP under the control of the human GFAP promoter²¹ as well as

CX₃CR1-EGFP mice expressing EGFP in microglia²². For details of surgical preparation, see **Supplementary Methods**.

Two-photon microscopy. Two-photon imaging in intact neocortex was done using a custom-built two-photon laser scanning microscope equipped with two fluorescence-detection channels. Laser wavelength varied in the range between 840 and 890 nm. Movement artifacts associated with the animal's heartbeat were overcome by triggering image acquisition from the heartbeat (for more details, see **Supplementary Methods**).

Labeling procedures. All labeling procedures were performed under anesthesia and with head fixation.

For *in vivo* labeling of cortical astrocytes, SR101 (Molecular Probes or Sigma) was dissolved in extracellular saline and briefly (1–5 min) applied either directly to exposed neocortical surface or on top of the craniotomy filled with 1.5% agar. In a few experiments, SR101 was locally pressure-ejected from a micropipette. Typical concentrations used were in the range of 25–100 μ M. After surface application, the craniotomy was rinsed repeatedly using prewarmed extracellular saline.

For the counter-immunostaining experiments, 100–500 μ M Texas Red-hydrizide (Molecular Probes), a paraformaldehyde-fixable analog of SR101, was applied to the cortical surface *in vivo* as described above. After rinsing, the dye was allowed to be taken up by cortical astrocytes for 50–70 min before transcardial perfusion.

Multicell bolus loading of layer 2/3 cells with calcium indicator was performed as described previously¹⁸. Briefly, Oregon Green 488 BAPTA-1 AM (Molecular Probes) was dissolved in DMSO plus 20% Pluronic F-127 (Molecular Probes) and then diluted with normal rat Ringer solution (NRR: 135 mM NaCl, 5.4 mM KCl, 5 mM HEPES, 1.8 mM CaCl₂, pH adjusted to 7.2 with NaOH) to a final concentration of 0.5–1 mM. This dye was then pressure-ejected through a micropipette using a short pressure pulse (1 min, 0.3–0.7 bar). This resulted in temporally stable, but nonspecific, labeling of cells (neurons and glial cells) with calcium indicator within approximately 300 μ m around the injection site.

Blood plasma was stained by tail-vein injection⁴⁷ of FITC-labeled dextran (77 kDa, 5% (w/v) in NRR, 0.1–0.2 ml; Sigma).

Tissue fixation and immunostaining. Animals were transcardially perfused with 4% paraformaldehyde in 0.1 M sodium phosphate buffer (pH 7.2). Brains were kept in fixative for 1–2 d. Coronal brain vibratome (Campden) sections 60 μ m thick were immunostained for S-100 β and CNPase as described²⁶ (for details, see **Supplementary Methods**). For immunostaining of the neuron-specific protein NeuN, slices were treated with 5% normal goat serum (NGS) and 1% Triton X-100 in PBS for 60 min, and then incubated overnight at 4 °C in 1% NGS and 0.3% Triton X-100 in PBS with antibody to NeuN (anti-NeuN; mouse monoclonal; 1:1,000; Chemicon). After three washing steps, slices were incubated with a FITC-conjugated secondary antibody (1:200; Dianova) in 1% NGS and 0.3% Triton X-100 in PBS for 2 h.

Data analysis. Maximum intensity projections and analysis of astrocyte distribution were performed on image stacks using custom-written macros in NIH Image. Volume densities were evaluated by counting cells within layer 1 or layer 2/3 and dividing by the analysis volume (at least 0.1 \times 0.1 \times 0.1 mm³). Radial

density was analyzed by calculating the distances r between all labeled cells within a volume of 0.3 mm side length, calculating the histogram (bin width 3 μm) and then dividing the histogram by $4\pi r^2$.

Calcium transients were measured using 64×128 pixel scans with 1-ms line scan duration (15-Hz frame rate). Fluorescence was averaged over cell body areas and expressed as relative fluorescence changes ($\Delta F/F$) after subtraction of background fluorescence from a neighboring region. All data are presented as mean \pm s.e.m.

Note: Supplementary information is available on the Nature Methods website.

ACKNOWLEDGMENTS

We thank J.R. Wolff for comments on the manuscript, S. Jung and D.R. Littman for providing the green fluorescent microglial mouse line, M. Kaiser for expert technical assistance, V. Grinevich for help with the antibody staining and B. Sakmann for generous support. A.N. was supported by a predoctoral fellowship of the Boehringer Ingelheim Fonds.

COMPETING INTERESTS STATEMENT

The authors declare that they have no competing financial interests.

Received 2 June; accepted 26 August 2004

Published online at <http://www.nature.com/naturemethods/>

- Fields, R.D. & Stevens-Graham, B. Neuroscience—New insights into neuron-glia communication. *Science* **298**, 556–562 (2002).
- Haydon, P.G. Glia: listening and talking to the synapse. *Nat. Rev. Neurosci.* **2**, 185–193 (2001).
- Bezzi, P. & Volterra, A. A neuron-glia signalling network in the active brain. *Curr. Opin. Neurobiol.* **11**, 387–394 (2001).
- Beattie, E.C. *et al.* Control of synaptic strength by glial TNF α . *Science* **295**, 2282–2285 (2002).
- Kang, J., Jiang, L., Goldman, S.A. & Nedergaard, M. Astrocyte-mediated potentiation of inhibitory synaptic transmission. *Nat. Neurosci.* **1**, 683–692 (1998).
- Pfrieger, F.W. & Barres, B.A. Synaptic efficacy enhanced by glial cells in vitro. *Science* **277**, 1684–1687 (1997).
- Cornellbell, A.H., Finkbeiner, S.M., Cooper, M.S. & Smith, S.J. Glutamate induces calcium waves in cultured astrocytes—long-range glial signaling. *Science* **247**, 470–473 (1990).
- Dani, J.W., Chernjavsky, A. & Smith, S.J. Neuronal activity triggers calcium waves in hippocampal astrocyte networks. *Neuron* **8**, 429–440 (1992).
- Zonta, M. *et al.* Neuron-to-astrocyte signaling is central to the dynamic control of brain microcirculation. *Nat. Neurosci.* **6**, 43–50 (2003).
- Simard, M., Arcuino, G., Takano, T., Liu, Q.S. & Nedergaard, M. Signaling at the gliovascular interface. *J. Neurosci.* **23**, 9254–9262 (2003).
- Nedergaard, M., Ransom, B. & Goldman, S.A. New roles for astrocytes: redefining the functional architecture of the brain. *Trends Neurosci.* **26**, 523–530 (2003).
- Denk, W., Strickler, J.H. & Webb, W.W. Two-photon laser scanning fluorescence microscopy. *Science* **248**, 73–76 (1990).
- Zipfel, W.R., Williams, R.M. & Webb, W.W. Nonlinear magic: multiphoton microscopy in the biosciences. *Nat. Biotechnol.* **21**, 1369–1377 (2003).
- Helmchen, F. & Denk, W. New developments in multiphoton microscopy. *Curr. Opin. Neurobiol.* **12**, 593–601 (2002).
- Ragan, T.M., Huang, H. & So, P.T.C. *In vivo* and *ex vivo* tissue applications of two-photon microscopy (eds. Marriott, G. & Parker, I.) in *Biophotonics Pt. B* Vol. 361, 481–505 (Academic Press, San Diego, 2003).
- Svoboda, K., Denk, W., Kleinfeld, D. & Tank, D.W. *In vivo* dendritic calcium dynamics in neocortical pyramidal neurons. *Nature* **385**, 161–165 (1997).
- Lendvai, B., Stern, E.A., Chen, B. & Svoboda, K. Experience-dependent plasticity of dendritic spines in the developing rat barrel cortex *in vivo*. *Nature* **404**, 876–881 (2000).
- Stosiek, C., Garaschuk, O., Holthoff, K. & Konnerth, A. *In vivo* two-photon calcium imaging of neuronal networks. *Proc. Natl. Acad. Sci. USA* **100**, 7319–7324 (2003).
- Helmchen, F. & Waters, J. Ca²⁺ imaging in the mammalian brain *in vivo*. *Eur. J. Pharmacol.* **447**, 119–129 (2002).
- Zhuo, L. *et al.* Live astrocytes visualized by green fluorescent protein in transgenic mice. *Dev. Biol.* **187**, 36–42 (1997).
- Nolte, C. *et al.* GFAP promoter-controlled EGFP-expressing transgenic mice: a tool to visualize astrocytes and astrogliosis in living brain tissue. *Glia* **33**, 72–86 (2001).
- Jung, S. *et al.* Analysis of fractalkine receptor CX₃CR1 function by targeted deletion and green fluorescent protein reporter gene insertion. *Mol. Cell. Biol.* **20**, 4106–4114 (2000).
- Privat, A., Gimenez-Ribotta, M. & Ridet, J.-L. Morphology of astrocytes. in *Neuroglia* (eds. Ransom, B.R. & Kettenmann, H.) 3–22 (Oxford University Press, Oxford, 1995).
- Ehinger, B., Zucker, C.L., Bruun, A. & Adolph, A. *In vivo* staining of oligodendroglia in the rabbit retina. *Glia* **10**, 40–48 (1994).
- Matthias, K. *et al.* Segregated expression of AMPA-type glutamate receptors and glutamate transporters defines distinct astrocyte populations in the mouse hippocampus. *J. Neurosci.* **23**, 1750–1758 (2003).
- Grass, D. *et al.* Diversity of functional astroglial properties in the respiratory network. *J. Neurosci.* **24**, 1358–1365 (2004).
- Diers-Fenger, M., Kirchhoff, F., Kettenmann, H., Levine, J.M. & Trotter, J. AN2/NG2 protein-expressing glial progenitor cells in the murine CNS: isolation, differentiation, and association with radial glia. *Glia* **34**, 213–228 (2001).
- Wallraff, A., Odermatt, B., Willecke, K. & Steinhauser, C. Distinct types of astroglial cells in the hippocampus differ in gap junction coupling. *Glia* **48**, 36–43 (2004).
- Wolff, J.R. & Chao, T.I. Cytoarchitectonics of non-neuronal cells in the central nervous system. in *Non-Neuronal Cells in the Nervous System: Function and Dysfunction. I. Structure, Organization, Development, and Regeneration Part 1* (ed. Hertz, L.) 1–51 (Elsevier, New York, 2004).
- Araque, A., Carmignoto, G. & Haydon, P.G. Dynamic signaling between astrocytes and neurons. *Annu. Rev. Physiol.* **63**, 795–813 (2001).
- Verkhatsky, A. & Kettenmann, H. Calcium signalling in glial cells. *Trends Neurosci.* **19**, 346–352 (1996).
- Charles, A.C., Merrill, J.E., Dirksen, E.R. & Sanderson, M.J. Intercellular signaling in glial cells—calcium waves and oscillations in response to mechanical stimulation and glutamate. *Neuron* **6**, 983–992 (1991).
- Pasti, L., Volterra, A., Pozzan, T. & Carmignoto, G. Intracellular calcium oscillations in astrocytes: a highly plastic, bidirectional form of communication between neurons and astrocytes *in situ*. *J. Neurosci.* **17**, 7817–7830 (1997).
- Hirase, H., Qian, L., Bartho, P. & Buzsaki, G. Calcium dynamics of cortical astrocytic networks *in vivo*. *PLoS Biology* **2**, 494–499 (2004).
- Waters, J., Larkum, M., Sakmann, B. & Helmchen, F. Supralinear Ca²⁺ influx in dendritic tufts of layer 2/3 neocortical pyramidal neurons *in vitro* and *in vivo*. *J. Neurosci.* **23**, 8558–8567 (2003).
- Lichtman, J.W., Wilkinson, R.S. & Rich, M.M. Multiple innervation of tonic endplates revealed by activity-dependent uptake of fluorescent probes. *Nature* **314**, 357–359 (1985).
- Keifer, J., Vyas, D. & Houk, J.C. Sulforhodamine labeling of neural circuits engaged in motor pattern generation in the *in vitro* turtle brainstem-cerebellum. *J. Neurosci.* **12**, 3187–3199 (1992).
- Arieli, A., Shoham, D., Hildesheim, R. & Grinvald, A. Coherent spatiotemporal patterns of ongoing activity revealed by real-time optical imaging coupled with single-unit recording in the cat visual cortex. *J. Neurophysiol.* **73**, 2072–2093 (1995).
- Petersen, C.C.H., Grinvald, A. & Sakmann, B. Spatiotemporal dynamics of sensory responses in layer 2/3 of rat barrel cortex measured *in vivo* by voltage-sensitive dye imaging combined with whole-cell voltage recordings and neuron reconstructions. *J. Neurosci.* **23**, 1298–1309 (2003).
- Safranyos, R.G.A., Caveney, S., Miller, J.G. & Petersen, N.O. Relative roles of gap junction channels and cytoplasm in cell-to-cell diffusion of fluorescent tracers. *Proc. Natl. Acad. Sci. USA* **84**, 2272–2276 (1987).
- Willis, C.L. *et al.* Focal astrocyte loss is followed by microvascular damage, with subsequent repair of the blood-brain barrier in the apparent absence of direct astrocytic contact. *Glia* **45**, 325–337 (2004).
- Kim, J. *et al.* Sindbis vector SINrep(nsP2S(726)): a tool for rapid heterologous expression with attenuated cytotoxicity in neurons. *J. Neurosci. Methods* **133**, 81–90 (2004).
- Feng, G. *et al.* Imaging neuronal subsets in transgenic mice expressing multiple spectral variants of GFP. *Neuron* **28**, 41–51 (2000).
- Ullian, E.M., Sapperstein, S.K., Christopherson, K.S. & Barres, B.A. Control of synapse number by glia. *Science* **291**, 657–661 (2001).
- Parpura, V. *et al.* Glutamate-mediated astrocyte neuron signaling. *Nature* **369**, 744–747 (1994).
- Nedergaard, M. Direct signaling from astrocytes to neurons in cultures of mammalian brain cells. *Science* **263**, 1768–1771 (1994).
- Kleinfeld, D. & Denk, W. Two-photon imaging of neocortical microcirculation. in *Imaging Neurons: A Laboratory Manual* (eds. Yuste, R., Lanni, F. & Konnerth, A.) 23.1–23.15 (Cold Spring Harbor Press, Cold Spring Harbor, New York, USA, 1999).